Nuclear Engineering and Design 239 (2009) 308–319

Contents lists available at ScienceDirect

Nuclear Engineering and Design

journal homepage: www.elsevier.com/locate/nucengdes

EBaLM-THP – A neural network thermohydraulic prediction model of advanced nuclear system components

Artit Ridluan[a,*], Milos Manic[b], Akira Tokuhiro[a]

[a] Nuclear Program, Department of Mechanical Engineering, University of Idaho, Idaho Falls, ID 83402-1575, USA
[b] Department of Computer Science, University of Idaho, Idaho Falls, ID 83402-1575, USA

ARTICLE INFO

Article history:
Received 16 May 2008
Received in revised form 16 October 2008
Accepted 31 October 2008

Keywords:
Neural network
Error-back propagation
Levenberg–Marquardt
Design optimization
Heat exchanger
PCHE
Supercritical CO_2
Thermohydraulic performance

ABSTRACT

In lieu of the worldwide energy demand, economics and consensus concern regarding climate change, nuclear power – specifically near-term nuclear power plant designs are receiving increased engineering attention. However, as the nuclear industry is emerging from a lull in component modeling and analyses, optimization for example using ANN has received little research attention. This paper presents a neural network approach, EBaLM, based on a specific combination of two training algorithms, error-back propagation (EBP), and Levenberg–Marquardt (LM), applied to a problem of thermohydraulics predictions (THPs) of advanced nuclear heat exchangers (HXs).

The suitability of the EBaLM-THP algorithm was tested on two different reference problems in thermohydraulic design analysis; that is, convective heat transfer of supercritical CO_2 through a single tube, and convective heat transfer through a printed circuit heat exchanger (PCHE) using CO_2. Further, comparison of EBaLM-THP and a polynomial fitting approach was considered. Within the defined reference problems, the neural network approach generated good results in both cases, in spite of highly fluctuating trends in the dataset used. In fact, the neural network approach demonstrated cumulative measure of the error one to three orders of magnitude smaller than that produce via polynomial fitting of 10th order.

1. Introduction

In order to meet the increasing national (US) and global energy (electricity) demands and simultaneously address growing consensus concern with respect to climate change (thus curbing GHGs – greenhouse gases), it is evident that we need to further develop nuclear power and alternative energy source, while reducing our current dependence on foreign oil. Only a renaissance in nuclear power can meet the large demand for baseload power in the United States (Southworth et al., 2003).

To meet both the new technical and public acceptance criteria, next generation, "Generation IV", nuclear power plants (NPPs) have to be *safe, economically competitive, proliferation-proof,* and *environmentally friendly*. Specifically, the US Department of Energy (DOE) is leading a number of initiatives, including the Next Generation Nuclear Plant (NGNP) project (Schultz and Nigg, 2004), also known as the very high temperature (gas-cooled) reactor (VHTR). Congressional mandate for the VHTR to be operational by 2021 with possible demonstration of a hydrogen generating plant has initiated various engineering design studies on both the NPP and secondary plant components.

For the NGNP-VHTR or any other higher temperature energy system, an power conversion system using an efficient heat exchanger (HX) is key to overall plant efficiency, as well as availability of process heat (i.e. for hydrogen production). Ideally, the functional need for the HX needs to be compact (to minimize material costs) yet thermal efficient is a non-linear and multi-dimensional exercise in parametric design optimization. In the nuclear industry, traditional design engineering has relied upon trial-and-error, iterative methods with design constraints siding on the side of conservatism with respect to margins of safety in operation and off-normal anticipated and unanticipated scenarios. However, we expect these practices to change; that is, design conservatism will be reduced in search of efficiency in system performance, while meeting regulatory (licensing) compliance. This research paper thus presents a specific artificial neural network (ANN) model called error-back propagation (EBP) and Levenberg–Marquardt-thermal–hydraulic prediction (EBaLM-THP), to support a design optimization of a key component in Generation IV NPPs, namely the printed circuit heat exchanger (PCHE) (Lillo, 2005).

* Corresponding author at: Nuclear Program, Department of Mechanical Engineering, University of Idaho, 1776 Science Drive, Idaho Falls, ID 83402-1575, USA. Tel.: +1 208 282 7714; fax: +1 208 282 7950.
E-mail address: aridluan@vandals.uidaho.edu (A. Ridluan).

0029-5493/$ – see front matter © 2008 Elsevier B.V. All rights reserved.
doi:10.1016/j.nucengdes.2008.10.027

Nomenclature

d_{op}	desired output
f	activation function of single neuron
f'	derivative of activation function of single neuron
$F\{z_p\}$	activation function of several neurons
$F'\{z_p\}$	derivative of non-linear function activation function of several neurons
g	gradient
H	Hessian
J	Jacobian
net	weighted sum of input
o	single neuron output
o_{op}	network outputs
TE	total error
w_i	neural weight
w_b	bias weight
Δw	weight change
x_i	neural net input
z_p	neuron output

Design analysis of heat exchanger is well documented in texts such as Incropera et al. (2007), as well as Shah and Sekulic (2003). Zig-zag micro-channel flow configuration with CO_2 as the heat transfer medium under near-to-critical conditions adds both non-linearity and complexity to the design analyses. As noted, existing thermal–hydraulic analyses and design optimization methods are based on a number of assumptions; thus simplifying the approach. However, the thermophysical properties (c_p, ρ, k, α and related) change significantly over a small temperature/pressure range near the critical point (NIST) and there is some evidence that for characteristic flow length under 1 mm, the hydrodynamics deviate from conventional analyses.

The non-linear thermophysical properties, as well as micro-channel flow and operating parameters suggest using an artificial neural network approach as a potential "tool" to facilitate the present design optimization task, especially to supplement computational fluid dynamics (CFDs) based modeling of the design in question.

The ANN approach has been considered in limited reported literature in nuclear science and technology. For example, Eryurek and Upadhyaya (1990) studied the possibility of employing neural network to model the signals from a commercial power plant and the experimental breeder reactor-II (EBR-II). Roh et al. (1991) developed a system of thermal power prediction in nuclear power plant by combining a neural network with a signal validation model. Further, Guo and Uhrig (1992) applied a hybrid type of neural networks to predict the heat rate, as linked to nuclear power plant performance. Boroushaki et al. (2005) applied cellular neural network (CNN) to simulate reactor core kinetics. Guanghui et al. (2003) trained artificial neural networks to predict the critical heat flux (CHF) under low pressure and oscillating conditions for both natural and forced circulation. Garg et al. (2007) applied multilayer perceptron (MLP) and radial basis function (RBF) neural networks to predict thermo-hydraulics of natural circulation boiling water reactor. Finally, Vaziri et al. (2007) applied RBF and MLP neural networks to also predict the CHF. ANN is evidently receiving consideration as a suitable in reactor analysis.

Artificial neural network has also been used to evaluate, design, and optimize the thermohydraulic performance of compact heat exchangers. Diaz and Sen (1999) developed and tested a several ANN structures with sigmoid activation function to predict the heat transfer rates for 1D conduction, 1D convection with one and two heat transfer coefficients, and a single-row plate-fin heat exchanger (PFHE). The authors used a back propagation (BP) algorithm, applied to train and test the networks of neuron. The results showed that the maximum error was less than 10% deviations. For the most complex application (plate-fin heat exchanger), 4–5–5–1 ANN configuration yielded the smallest standard deviation. Pacheco-Vega (2001) applied a feed-forward (FF) structure with sigmoid function to fin-plate type heat exchanger analysis for a refrigeration application. The NN was trained using BP algorithm. A root-mean square estimation indicated that error predicted by ANN is less than 1.5% relative to the experimental data and has the same degree of uncertainty of experiment. Additional details regarding experimental correlation and ANN model for steady-state performance of a plate-fin-tube heat exchanger is contained in Pacheco-Vega's dissertation (2002). Recently, Ping and Ling (2008) proposed using a combination of genetic algorithm (GA) and BP ANN to optimize the PFHE size and its capital cost. Ermis (2007) applied ANN to estimate heat transfer coefficient, pressure drop, and Nusselt number for a 15-channel configuration compact heat exchanger with staggered cylindrical and triangular ribs. The three-layer NN learning process was carried out by a feed-forward back propagation (FFBP) algorithm.

Although heat exchanger analysis via application of neural networks have been documented, these are mostly for extended surface-type, traditional heat exchangers with heat transfer media at conventional thermophysical conditions. Compact heat exchangers with micro-channels using supercritical fluids have yet to be investigated.

This paper demonstrates the predictive ability of an ANN-based approach to assess PCHE thermohydraulics with the heat transfer medium near or at critical conditions. The application is limited to supercritical carbon dioxide (CO_2) which has been identified as a suitable fluid. However, we first consider convective heat transfer through a single tube. Subsequently, a heat exchanger with multiple zig-zag micro-channels (PCHE) is considered.

2. Printed circuit heat exchanger

2.1. General description

PCHE was first introduced in Australia for refrigeration applications (ca 1985) (Feay, 1994). Subsequently since 1990 in the UK, the Heatric has continuously developed the design and extended the application of the PCHE. In recent times, the PCHE has been considered the key heat exchanger in the indirect Brayton cycle featured in many advanced nuclear systems, including the NGNP-VHTR (Lillo, 2005).

The PCHE consists of micro-channels acid etched into a zig-zag pattern on a plate as shown in Fig. 1(a and b). The plates are then diffusion bonded under high temperature and pressure. The resulting heat exchanger has very good thermal contact between the plates and these plates can be arranged into counter-current, co-current, cross-current or other combination and/or orientation as shown in Fig. 1(b) (Heatric website).

2.2. Thermohydraulic behavior

According to Li et al. (2006), supercritical carbon dioxide (SCO_2) is attractive if the PCHE functions as the NGNP secondary loop heat exchanger. To date, only few have reported research on the thermal–hydraulic performance of the PCHE using SCO_2. The reported works are by Van Meter (2008), Song (2007), Song et al. (2006), Nikitin et al. (2006), Tsuzuki et al. (2007), Lomperski et al. (2006) and Ishizuka et al. (2005). This paper presents an artificial

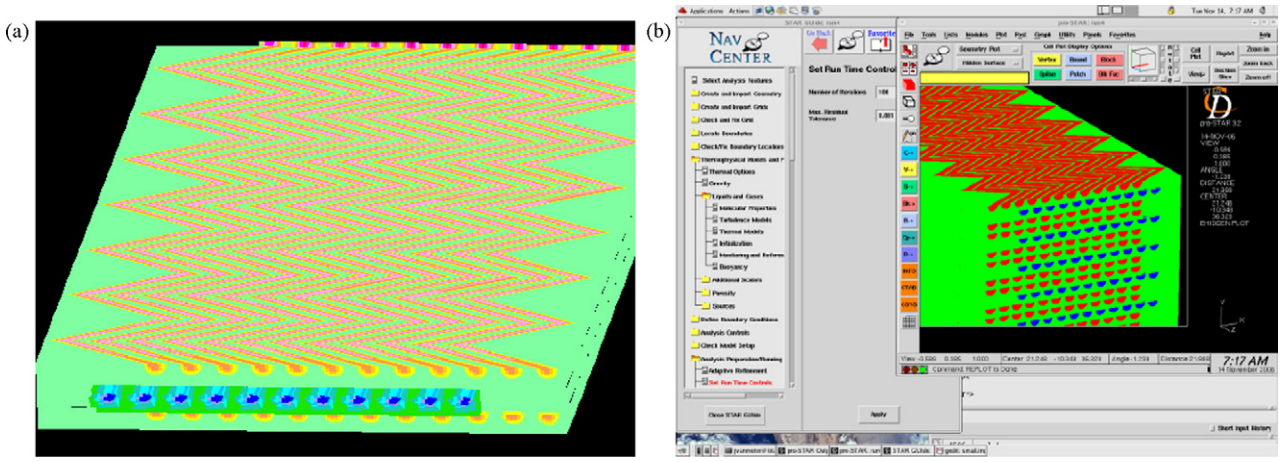

Fig. 1. The printed circuit heat exchanger configuration: (a) zig-zag micro-channels on a plate and (b) stacked plates. Both during geometric modeling using STAR-CD.

neural network-based thermohydraulic analysis of a generalized compact heat exchanger under consideration for an advanced nuclear system. The heat exchanger uses a supercritical fluid (a fluid near or at its critical point) to maximize its performance. The study here suggests an alternative modeling approach to thermal system component design optimization.

2.3. Experimental database

We selected two experiments to serve as our training and testing database for the present ANN application. These thermohydraulic datasets are characterized with respect to increasing flow configuration complexity for convective heat transfer.

The experimental dataset by He et al. (2005) is first described. He's group conducted experiments and numerical simulations of convective heat transfer in a vertical micro-channel with SCO_2 as heat transfer medium. They validated the simulations with experimental data under conditions noted in Table 1. He's experiments were carried out in a stainless steel (1CR189NT) vertical tube with an internal and external diameters 0.948 and 1.729 mm, respectively. The critical pressure range of SCO_2, is 8.5–9.5 MPa. The test section, 55 mm in length was heated by passing a low voltage alternating current. The experimental uncertainty was reported to be 11.3%. In the present work, we chose the following parameters from He's work: the inlet pressure (P_i), the inlet temperature (T_i), the mass flow rate ($\dot{m}$), the Reynolds number (Re), and the Buoyancy parameter (Bo). He et al. defined Bo as

$$Bo \equiv \frac{Gr^*}{Re^{3.425}Pr^{0.8}} \tag{1}$$

where Gr^* is the Grashof number, defined by

$$Gr^* \equiv \frac{\beta g D^4 q''_w}{\lambda \nu^2} \tag{2}$$

Here, Pr, β, λ, and ν are Prandtl number, coefficient of thermal expansion, thermal conductivity, and kinematic viscosity, respectively. The output is the wall heat flux, q''_w.

An additional experimental dataset for a PCHE using SCO_2 as reported by Ishizuka et al. (2005) was also referenced. The data from this work is listed in Table 2. The capacity of the PCHE reported by Ishizuka is 3 kW; each PCHE consists of 12 hot and 11 cold semi-circular, zig-zagged flow channel plates, made of SS316L. The zig-zag was defined by 115° and 100° for hot and cold plates, respectively. The cross-sectional areas of hot and cold channel are 0.0002 and 0.000092 m^2, respectively. An electrical heater was utilized to

Table 1
Thermohydraulic database (He et al., 2005).

Mass flow rate, $\dot{m}$ (kg/h)	Inlet temperature, T_i (°C)	Inlet pressure, P_i (MPa)	Reynolds number, Re	Buoyancy number, Bo	Wall heat flux, q''_w (kW/m^2)
1.48	32.7	9.59	9,237	936×10^{-10}	31,534
1.53	37.8	9.54	11,639	790×10^{-10}	31,194
1.49	39.6	9.5	12,629	796×10^{-10}	30,722
1.37	51	9.43	20,864	208×10^{-10}	29,400
1.69	32.8	9.52	10,641	1360×10^{-10}	71,843
1.6	36.1	9.42	11,474	1610×10^{-10}	71,703
1.63	40.9	9.57	14,765	1240×10^{-10}	70,242
1.65	48.3	9.49	23,417	367×10^{-10}	70,005
1.48	32.7	9.59	9,237	936×10^{-10}	31,534
1.71	32.7	9.49	10,761	719×10^{-10}	39,554
2.93	33.4	9.47	18,888	131×10^{-10}	45,561
3.45	31.7	9.55	20,972	62.1×10^{-10}	37,744
4.17	31	8.56	24,837	34×10^{-10}	39,558
4.06	33.4	8.57	29,255	37.5×10^{-10}	37,700
4.03	33.4	8.47	29,585	68.6×10^{-10}	66,583
4.08	33.3	8.51	29,558	99.2×10^{-10}	100,770
4.08	33.3	8.51	29,558	197×10^{-10}	200,000
4.06	33.4	8.57	29,255	9.96×10^{-10}	10,000
1.51	33.5	8.46	11,173	1160×10^{-10}	38,993
1.52	35	8.46	12,537	1100×10^{-10}	38,692
1.5	38.4	8.47	19,379	467×10^{-10}	36,287
1.49	44	8.48	24,138	174×10^{-10}	37,079

Table 2
Thermohydraulic database (Ishizuka et al., 2005).

Mass flow rate, G (kg/h)	Inlet hot CO_2 pressure, $P_{h,i}$ (MPa)	Inlet cold CO_2 pressure, $P_{c,i}$ (MPa)	Inlet hot CO_2 temperature, $T_{h,i}$ (°C)	Inlet cold CO_2 temperature, $T_{c,i}$ (°C)	Cold CO_2-sided pressure drop, DP_c (kPa)	Hot CO_2-sided pressure drop, DP_h (kPa)	Heat transfer, Q (kW)
42.8	2.26	6.59	280.1	107.8	34.93	9.96	2.067
52.6	2.22	6.53	280.2	107.8	53.52	15.23	2.539
79.6	2.5	7.34	279.9	107.9	93.07	26.66	3.860
66.2	2.5	7.38	279.7	107.9	70.34	20.29	3.210
55.9	2.48	7.47	279.8	107.9	49.47	14.60	2.710
45.3	2.56	7.45	279.6	107.9	36.83	10.50	2.196
33.5	2.49	7.44	279.8	107.9	20.09	5.99	1.624
74.9	2.54	8.35	279.9	107.9	73.22	24.18	3.661
66.6	2.58	8.24	279.9	107.9	61.49	19.72	3.259
55.6	2.56	8.27	279.9	108.0	44.65	14.48	2.720
44.0	2.54	8.31	279.9	108.1	28.03	9.23	2.151
83.3	2.99	9.48	280.0	108.1	79.17	25.63	4.120
72.0	3.0	9.49	280.1	108.1	61.09	19.72	3.558
60.7	3.05	9.54	280.1	108.1	44.40	14.13	3.004
48.6	3.06	9.5	280.1	108.1	29.68	9.34	2.410
87.0	3.23	10.09	280.1	108.2	80.35	25.91	4.324
76.3	3.33	10.04	279.9	108.3	64.62	20.07	3.798
63.8	3.31	10.06	280.8	108.1	46.39	14.44	3.177
52.1	3.34	10.08	280.1	108.2	32.83	10.13	2.601

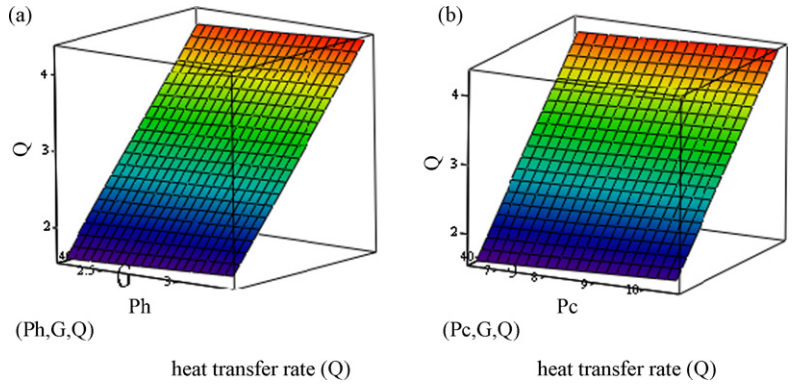

Fig. 2. 3D graphical representation of: (a) heat transfer rate Q vs. P_h and G and (b) heat transfer rate Q vs. P_c and G from data given in Table 2.

control the temperatures of CO_2. The pressure on each side and the pressure loss in PCHE was measured using a pressure gage transducer (±0.25% precision) and a differential pressure gage (±0.15% precision). The temperature was measured by using the copper-constantan thermocouples, ±0.15 °C accuracy. The flow rate was measured using both a turbine flow meter and the area flow meter with ±2% precision.

The hot ($P_{h,i}$), and cold ($P_{c,i}$) CO_2 inlet pressures, hot ($T_{h,i}$) and cold ($T_{c,i}$) inlet CO_2 temperatures, and mass flow rate (G), were considered as input factors that influenced three output parameters: the pressure drop through cold CO_2 side (DP_c); the pressure drop through hot CO_2 side (DP_h); and heat transfer (Q). A three-dimensional (3D) graphical representation of the dataset corresponding to Table 2 is given in Figs. 2 and 3 and depicts the linear

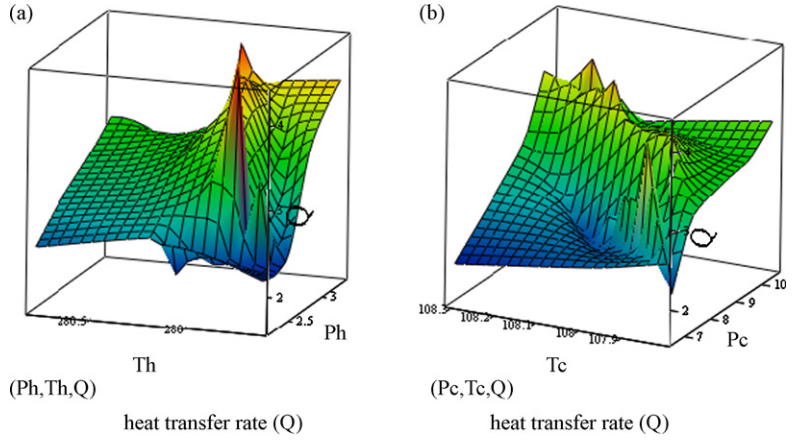

Fig. 3. 3D graphical representation of: (a) heat transfer rate Q vs. T_h and P_h (b) heat transfer rate Q vs. T_c and P_c from data given in Table 2.

to (very) non-linear nature of the dataset, based on the input variables. In fact, in Fig. 3, we see the sharp features (large gradients) in the 'functional space' as mapped. Needless to say, the relationship between input and output is non-linear.

2.4. Thermal system design and artificial neural networks

A brief summary of the ANN approach is given below. ANN and further, fuzzy approaches in engineering have matured such that developments are contained in texts such as Tsoukalas and Uhrig (1997). In thermohydraulics, Mi, Ishii, Tsoukalas and co-workers (1996, 1998, 2001) used a neural network approach for two-phase flow regime identification in vertical pipe-flow. The 'adaptability' of ANN in characterization of non-linear phenomena is evident; however, its acceptance as a research 'tool' is ongoing. We thus present a case here for convective heat transfer applications using supercritical fluids.

In traditional log-mean temperature difference (LMTD) heat exchanger analysis, the set of equations used to calculate the log-mean temperature, convective heat transfer correlation and overall heat transfer coefficient, are non-linear relationships. In fact, as the LMTD method assumes constant properties, HX analysis with supercritical heat transfer media introduces another element of non-linearity (Song, Van Meter, Song et al.). Thus, in the course of HX design via the LMTD method (or modified as needed for supercritical fluids), we undertake an iterative process to meet one or more objectives. Thus, similar to flow regime identification, there are input and output parameters, between which there exists a (known) set of equations which links one to the other. Further within the experimental realm, one must realize that there is not only non-linearity but 'noise' associated with quantification of phenomena (spatio-temporal changes in impedance in the case of Ishii; heat transfer and pressure drop in the present case). Thus if one can quantitatively reproduce or 'mimic' the non-linear character of a phenomena, and link this to physical design parameters, one can potentially facilitate the accurate design of thermal systems and components. The present work aims to demonstrate this ability (as did by Mi, Ishii, Tsoukalas and co-workers).

3. EBaLM-THP – a neural network algorithm for thermohydraulic prediction

Neural networks (ANN) are computational architectures constructed with a goal of mimicking biological neural networks. ANNs can contain several layers of neurons, which can be fully or partially connected.

A biological neuron is a computational unit which connects to other neurons via its interconnections (synapses), and receives the stimulated input via its inputs dendrites. A weighted sum of input signals (net value) is then typically compared against the threshold or certain activation function. An output signal produced in such a way is further transmitted via other synapses to other neurons.

To mimic a biological neuron, its artificial counterpart reproduces a similar functionality, i.e. calculates a weighted sum of input signals and compares it against the activation function (or threshold), as shown in Fig. 4. If the weighted sum of input signals (*net*) is above the threshold, a neuron will emit the output signal. The general neuron functionality can be expressed in conventional summation as

$$net = w_i x_i + w_b \tag{3}$$

where x_i is a neural net input, while w_i and w_b are neural and bias weights.

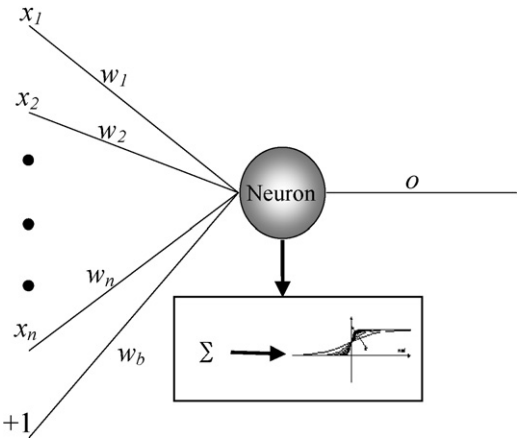

Fig. 4. Single artificial neuron with input and output connection.

An output of a neuron (o) is defined as

$$o = f(net) \tag{4}$$

where f represents the activation function.

Typically, the unipolar sigmoid activation function such as

$$f(net) = \frac{1}{1 + \exp(-net)} \tag{5}$$

is used.

Neural network architectures will here be described as "ANN m–n–k", where m, n, and k represent the number of neuron in the input, hidden, and output layers, respectively (Fig. 5). Such architecture will be used throughout this paper. For instance, ANN 7–5–1 means that the neural net is composed of an input, hidden, and output layers as follows: 7 neurons in the input layer; 5 neurons in the hidden layer; and 1 output layer.

The EBaLM-THP algorithm for thermohydraulic prediction modeling of the advance nuclear system component presented in this paper was implemented in Matlab 6.0 environment. The EBaLM-THP algorithm combines the two specific neural network training algorithms, EBP and Levenberg–Marquardt (LM). Here the former one is used for a specific error propagation, the latter one is used for training of specific neurons. In this way, the two expected advantages are combined; that is, the robustness of EBP with the speed of LM algorithm.

Physics-based modeling and corresponding experiments are undeniably the best approach to prediction modeling, when available. However, in case where such practices are difficult or (too) costly, the practical approach to modeling via ANN represents a

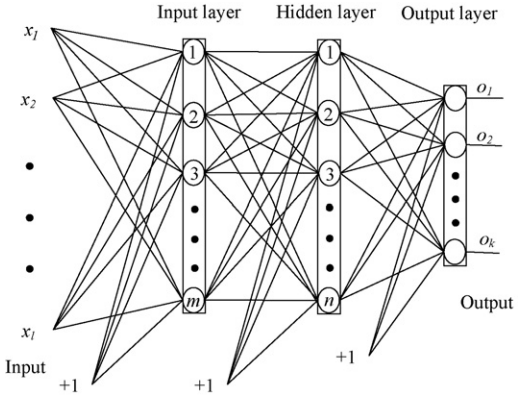

Fig. 5. An artificial neural architecture with input and output connection.

viable alternative. We also note that the neural network approach requires the existence of (accessible) data. In case where experimental data is not available, the development of physics-based model is preferred over an ANN approach without an appropriate dataset.

Thermohydraulic modeling, especially in the design of nuclear system components requires time-consuming iterations (trial-and-error). This is partly because a closed form solution rarely exists and/or physical models not only take time but call for reasonable understanding of key phenomena. The strength of the EBaLM-THP neural network algorithm is in its ability to learn and optimize the complex interdependencies of the variables, existing in the thermohydraulic prediction modeling. This is achieved through a particular neural network architecture on which the specific combination of two learning algorithms, namely, error-back propagation and Levenberg–Marquardt, algorithms was applied.

Here we presented the EBaLM-THP neural network algorithm based on a "data driven" approach. Performance analysis is strictly based on the total error calculated from the dataset available. The training process is executed as follows. The initial dataset is divided in two equal sets; one was used for training, and the other, used for testing of the presented model. As will be shown, the result presented in terms of total error, showed better agreement with the data (relative to a common polynomial 'trendline' approximation).

At this juncture, the benefits of this approach appears as follows: (1) trained neural networks are capable of predicting 'system' characteristics in situations beyond the training dataset, as long as the 'consistency' of the data is preserved. Data consistency here is beyond the scope of the research; we anticipate that it will be considered; (2) if one can have confidence in ANN-based models, one can potentially better understand the underlying physics via consideration of small variations in both the input and output parameter; (3) if one can have confidence in the ANN-based models, one can adjust the experimental parameters to elucidate physical parameters that may or may not yield similar non-linear characteristics.

Historically, the EBP algorithm was the first approach that countered a negative viewpoint on artificial neural networks via a text (Minsky and Papert, 1969). In fact, the EBP work by Werbos (1994) represented a real breakthrough in ANN research; he introduced a multilayer network approach and sigmoid activation functions, thereby solving linearly non-separable problems, as well as other complex, highly non-linear and multidimensional problems.

The main concept behind EBP is that calculated errors are propagated back after the transmitted inputs from the first layer have reached the output layer. During the backward propagation of errors, weights of neurons that produced the error are modified accordingly, going back from one layer to another, as illustrated in Fig. 6. Therefore, the EBP algorithm consists of two phases as follows: a forward propagation and then, backward propagation phase. In order to minimize the output error, the weight change is applied to the gradient change as

$$\Delta w_{pi} \sim 2\sum_{p=1}^{np}[(d_p - o_p)F'\{z_p\}f'(net_p)x_{pi}] \tag{6}$$

Here, Eq. (6) is extended to all weights applied to neurons. The associated EBP diagram is presented in Fig. 7. Equally,

$$\Delta w_p = \alpha\sum_{o=1}^{no}\sum_{p=1}^{np}[(d_{op} - o_{op})F'\{z_p\}f'(net_p)x_p] \tag{7}$$

where x_p represent network input pattern while d_{op}, z_p, and o_{op} are desired, neuron, and network outputs, respectively. The term, $f'(net_p)$, is the derivative of activation function f with respect to the

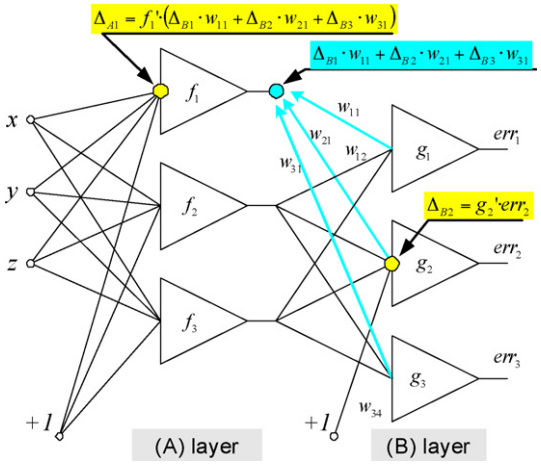

Fig. 6. Diagram of the propagation of error in EBP algorithm (Zurada, 1992).

neuron net value (net_p) and $F'\{z_p\}$ is the derivative of non-linear function $F\{z_p\}$ based on activation function of several neurons with respect to the neuron output (z_p)

The adjustment of weights on neurons plays a key role in ANN training. Such weighting update is typically described as

$$w_{k+1} = w_k + \Delta w_k \tag{8}$$

where w_k and Δw_k are weights and weight increment in iteration k, while w_{k+1} is updated weight in the following, $k+1$ iteration.

The neuron training process is executed using Levenberg–Marquardt (LM) algorithm (Levenberg, 1944; Marquardt, 1944). The weight increment equation of LM algorithm is derived from Newton method and written as

$$\Delta w_k = A_k^{-1} g \tag{9}$$

where A and g are Hessian and gradient such as:

$$A \cong 2J_k^J J_k \tag{10}$$

and

$$g = 2J_k^J e \tag{11}$$

Here, e is the error vector, while J is the Jacobian of the partial derivative of error with respect to each of the weights. The Hessian and gradient can be written in the matrix form as follows:

$$A = \begin{bmatrix} \frac{\partial^2 E}{\partial w_1^2} & \frac{\partial^2 E}{\partial w_2 \partial w_1} & \cdots & \frac{\partial^2 E}{\partial w_n \partial w_1} \\ \frac{\partial^2 E}{\partial w_1 \partial w_2} & \frac{\partial^2 E}{\partial w_2^2} & \cdots & \frac{\partial^2 E}{\partial w_n \partial w_2} \\ \vdots & \vdots & \ddots & \vdots \\ \frac{\partial^2 E}{\partial w_1 \partial w_n} & \frac{\partial^2 E}{\partial w_2 \partial w_n} & \cdots & \frac{\partial^2 E}{\partial w_n^2} \end{bmatrix} \quad \text{and} \quad g = \begin{bmatrix} \frac{\partial E}{\partial w_1} \\ \frac{\partial E}{\partial w_2} \\ \cdots \\ \frac{\partial E}{\partial w_n} \end{bmatrix}$$

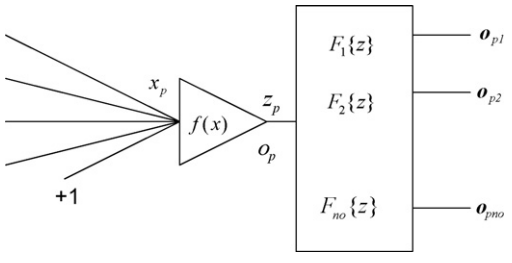

Fig. 7. Diagram of EBP algorithm with multi-outputs.

To anticipate issues with ill-defined Jacobian matrix, an identity matrix, I, can be introduced that results in the following version of weighting update Eq. (8), that is:

$$w_{k+1} = w_k - (J_k^T J_k + \mu I)^{-1} J_k^T e \tag{12}$$

The LM algorithm combines the speed of the Newton algorithm with the stability of the steepest decent method. The LM algorithm (12) calculates weights in subsequent iterations. It is important to note that the parameter μ controls the LM algorithm. For $\mu = 0$, the LM algorithm reduces to the Gauss–Newton method while for very large μ, the LM algorithms is reduced to the steepest decent.

4. Simulation results

As noted, testing was undertaken on two different thermo-hydraulic cases (CASE 1 and CASE 2) on heat exchanger using supercritical CO_2 as the heat transfer media. The first problem was convective heat transfer in a mini-tube; the second, convective heat transfer in multiple, zig-zagged micro-channel based, PCHE. Finally, a comparative analysis of ANN versus polynomial fitting (PF) was undertaken. The datasets were equally divided into training and testing datasets.

4.1. CASE 1: convective heat transfer CO_2 through a single tube

In the first example, EBaLM-THP algorithm was tested on a problem of supercritical CO_2 flow through a straight tube. One half of the data was used for training, the other half for testing. Training and testing datasets are illustrated in terms of heat flux (q''_w) versus temperature (T) in Fig. 8. All of values are normalized by the corresponding maximum values. That is, $T_{i,max} = 51\,^{\circ}C$ and $q''_{w,max} = 200,000\ \text{kw/m}^2$ both as noted by He et al. As shown, both the training and testing datasets fluctuate but are closely matched and bounded.

Twenty neural network structures were classified into four groups to investigate the predictive ability of EBaLM-THP algorithm. The performance of these ANN architectures is characterized here by the total error (TE); that is, the cumulative overall error of the dataset is defined as

$$TE = \sum_{p=1}^{np} [d_p - a_p]^2 \tag{13}$$

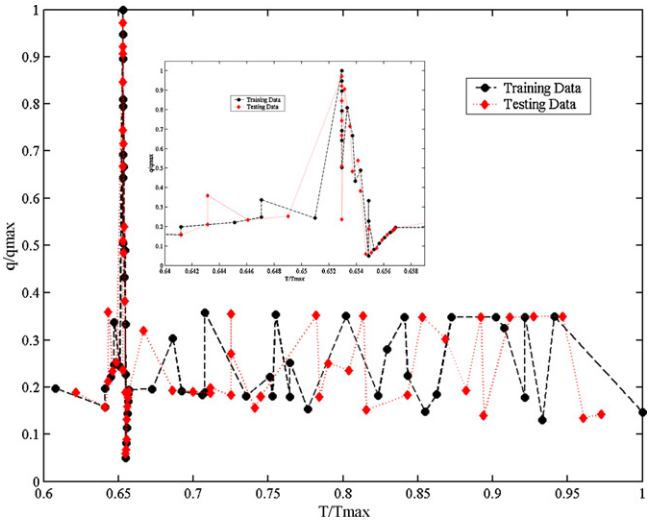

Fig. 8. Training and testing datasets.

Table 3
Total error of single tube thermohydraulic prediction.

Group 1 (five neurons in IL)		Group 3 (seven neurons in IL)	
Network	Total error	Network	Total error
ANN 5–3–1	1.295980084	ANN 7–3–1	0.450298264
ANN 5–5–1	0.954825917	ANN 7–5–1	1.158208468
ANN 5–6–1	1.458969153	ANN 7–6–1	2.725470938
ANN 5–7–1	0.683982214	ANN 7–7–1	2.662471685
ANN 5–8–1	0.989711546	ANN 7–8–1	0.730554961
Group 2 (six neurons in IL)		**Group 4 (eight neurons in IL)**	
Network	Total error	Network	Total error
ANN 6–3–1	3.503557982	ANN 8–3–1	0.450298264
ANN 6–5–4	0.764594655	ANN 8–4–1	1.158208468
ANN 6–6–1	0.294291329	ANN 8–5–1	2.725470938
ANN 6–7–1	0.500910836	ANN 8–6–1	2.662471685
ANN 6–8–1	2.879453675	ANN 8–7–1	0.730554961

where d_p and a_p are the reference (experimental) and actual data (ANN output), respectively.

The TE was calculated for various three-layered NN architectures and summarized in Table 3. The calculations with the number of layers different than three are not presented, because of the higher TE. Results were organized into groups, where the number of neurons in input layer (IL) is fixed, while the numbers of neurons in the second and third layers were varied. A graphical illustration of TE versus selected neural network architectures is presented in Fig. 9. For the architectures ANN 7–n–1 and ANN 8–n–1, the TE versus the total number of neurons is nearly identical.

We have learned that the initial weight associated with each neuron has an influence on the performance of ANN simulation. The initial weights were determined heuristically. The weights for ANN 6–6–1, ANN 8–4–1, ANN 7–5–1 and others were selected and then, their initial weights modified. The total error of the modified weights relative to the original, for each chosen ANN structure is given in Table 4.

A comparison between ANN predictions by ANN 8–4–1 with the new initial weight set versus experimental measurements is selected and graphically shown in Fig. 10.

Fig. 10 depicts the apparent effectiveness of ANN 6–6–1, ANN 7–5–1, and ANN 8–4–1 architectures. In spite of the highly fluc-

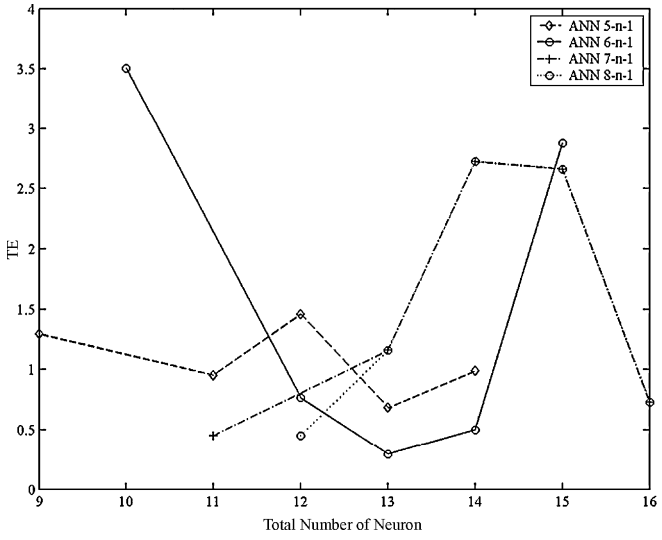

Fig. 9. The comparison of total error vs. total number of neuron for each group of ANN architectures.

Table 4
Modified total error of single tube thermohydraulic prediction.

Network	Previous total error	Modified total error
ANN 6–6–1	0.294291329	0.23138004
ANN 8–4–1	1.158208468	0.32930703
ANN 7–5–1	1.158208468	0.1976367

tuating data, these networks were able to successfully learn the behavior of the heat exchanger with supercritical CO_2.

4.2. CASE 2: convective heat transfer through PCHE

Similarly for PCHE one half of the complete dataset was used for training, while the rest was used for testing the EBaLM. The training and testing data for the PCHE is here plotted against mass flow rate (G), hot-sided pressure (P_h), and cold-sided pressure (P_c), and shown in Figs. 11–13, respectively. All of the values were normalized by the corresponding maximum values, as follows: DP_{cmax} = 93.07 kPa, G_{max} = 87 kg/h, DP_{hmax} = 26.66 kPa,

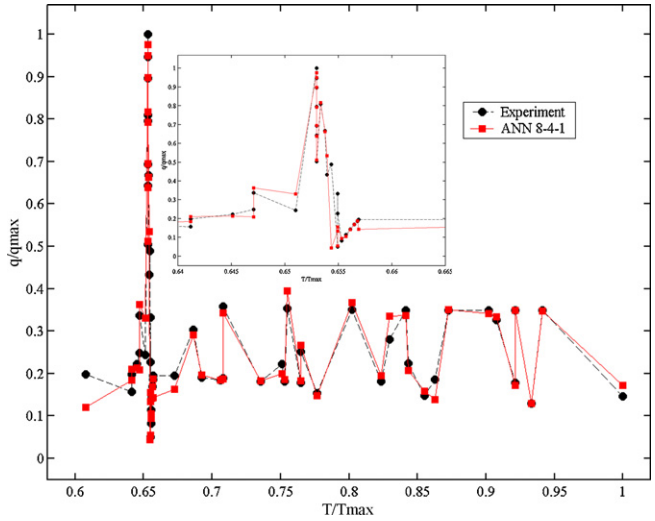

Fig. 10. The comparisons of experimental data vs. ANN outputs for ANN 8–4–1.

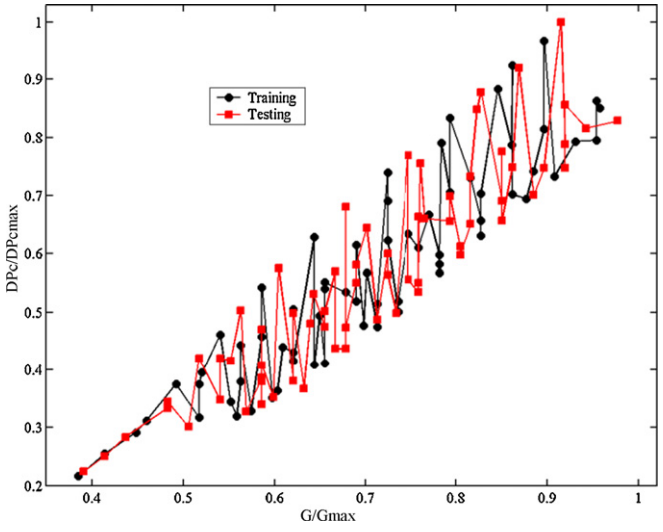

Fig. 11. The plots of training data and testing data for cold-sided pressure drop.

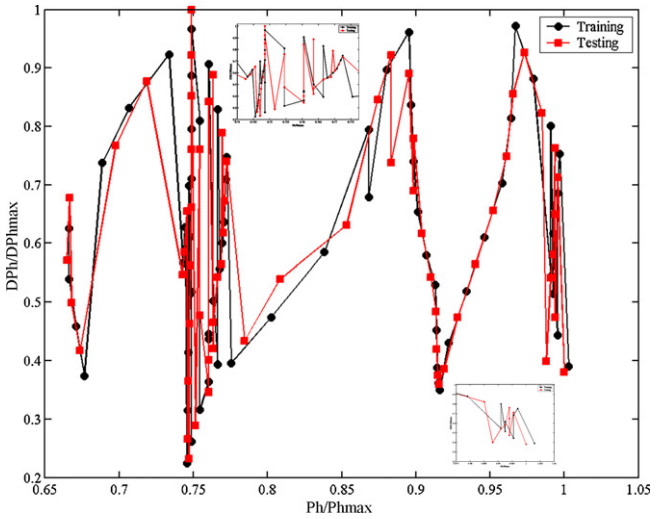

Fig. 12. The plots of training data and testing data for hot-sided pressure drop.

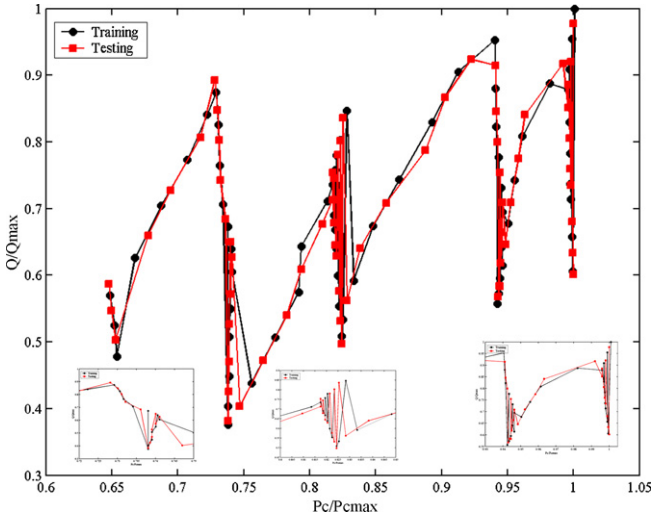

Fig. 13. The plots of: (a) training data and (b) testing data for heat transfer.

$P_{hmax,i}$ = 3.34 MPa, and Q_{max} = 4.324 kW. Though different to CASE 1, the test and training datasets again fluctuate and oscillate. In fact, there are sharp 'hi-and-low' changes as shown.

For the PCHE thermohydraulics, four neural network architectures were investigated and their performance measured using the *TE* Eq. (13). The performance of each ANN architecture is given in Table 5. We can see that ANN 7–5–3 and ANN 9–7–3 yielded the best results, while ANN 8–4–3 yielded relatively poorer results. It is evident that the PCHE experimental data reported by Ishizuka et al. (2005) is highly non-linear (Fig. 3). As indicated in Table 5, a larger number of neurons does not necessarily yield better per-

Table 5
Total error of PCHE thermohydraulic prediction.

Network	DP_c	DP_h	Q
ANN 7–5–3	0.00469135	0.006787571	0.002496384
ANN 7–7–3	0.01833685	0.051948002	0.12572272
ANN 8–4–3	0.08875032	0.18246256	0.093324986
ANN 9–7–3	0.01929302	0.007677054	0.002277966

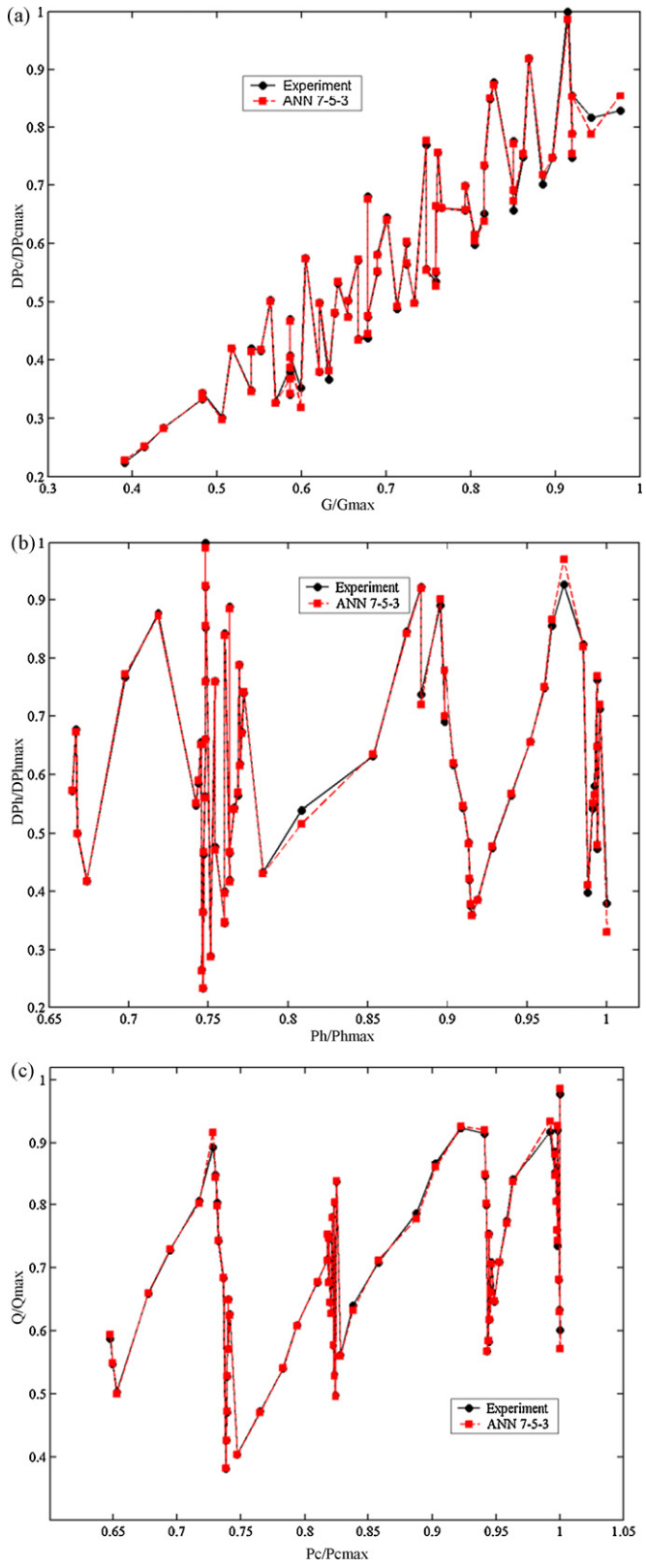

Fig. 14. The comparisons of experimental data vs. ANN 7–5–3 outputs for (a) cold-sided pressure drop, (b) hot-sided pressure drop and (c) heat transfer.

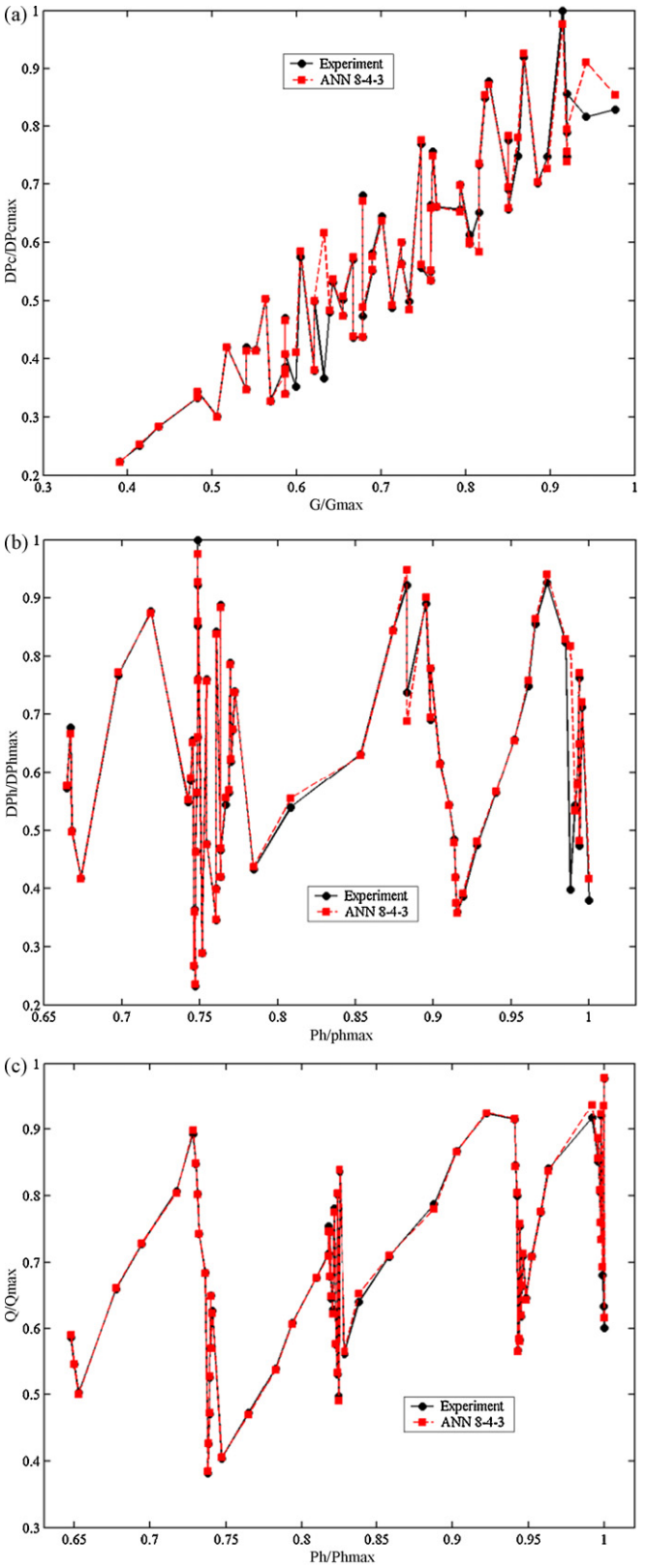

Fig. 15. The comparisons of experimental data vs. ANN 8–4–3 outputs for: (a) cold-sided pressure drop, (b) hot-sided pressure drop and (c) heat transfer.

formance. We also note that in CASE 2 (PCHE), the data does not exhibit 'jumps' as observed in CASE 1. Consequently, the *TE* in CASE 2 is lower than in CASE 1. As might be expected in a highly fluctuating 'signal' the error associated with modeling of such processes (peak in Fig. 10), is inherently higher than the error associated with less 'chaotic' processes (fluctuating but gradually varying or oscillating, as in Figs. 11–13). For example, the *TE* resulting from applying network architecture ANN 7–5–1 (CASE 1), is approximately 250% higher that the *TE* resulting from applying of ANN 7–5–3 architecture that was used in CASE 2. This shows that in spite of the fluctuating data, neural networks have the ability to 'adapt and learn' the thermohydraulic character of the PCHE.

A comparison of simulation, ANN 7–5–3, versus the experimental reference, for cold-sided pressure drop, hot-sided pressure drop, and heat transfer is shown in Fig. 14(a)–(c), respectively. We can see that the ANN results are generally in good agreement with the experimental data.

The simulation trends of the 8–4–3 ANN architecture, which has relatively poor performance, is presented in terms of the cold-sided pressure drop, hot-sided pressure drop, and heat transfer in Fig. 15(a)–(c), respectively. Even here, we can see that the neural network architecture, in fact for ANN '8–*n*–3' is in good agreement with the experimental reference. For example, the ANN 8–4–3 architecture (the one with the lowest prediction performance), the *TE* has good values, 0.088750320, 0.182462560, 0.093324986, for ΔP_c, ΔP_h, and Q, respectively.

4.3. Comparison of ANN versus polynomial fitting (FT)

To demonstrate the predictive ability of EBaLM, the ANN approach was also compared against a 10th order polynomial 'fit' (Matlab) of the reference conditions. A comparison of ANN versus the 10th degree polynomial for first example is shown in Fig. 16, while the second example is shown in Fig. 17(a)–(c).

As illustrated in Figs. 16 and 17, the EBaLM is 'superior' to the 10th polynomial as the polynomial essentially serves as a 'moving average' of the non-linear trend exhibited by the reference condition. It cannot in any way mimic the fluctuating nor oscillatory trend in the data. Meanwhile, ANN predicts many to most data points. For the first example, the total error of the 10th polynomial fitting was 2.299016210, while that of ANN 8–4–1 was a smaller 0.329307030. The computed total errors of 10th polyno-

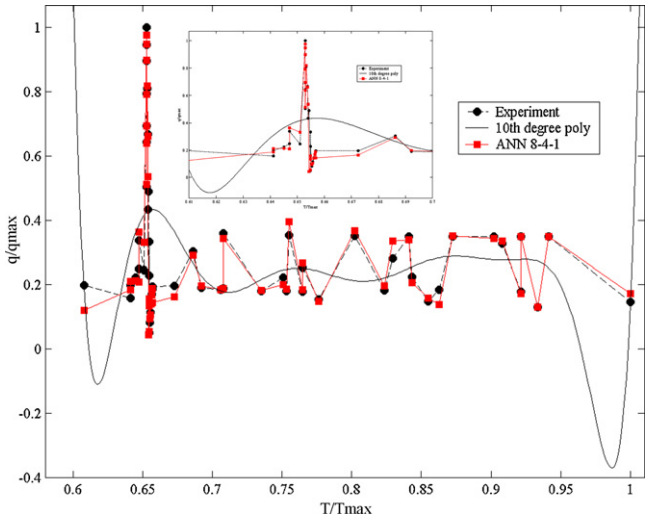

Fig. 16. The first example: the comparisons of ANN 8–4–1 vs. 10th order PF.

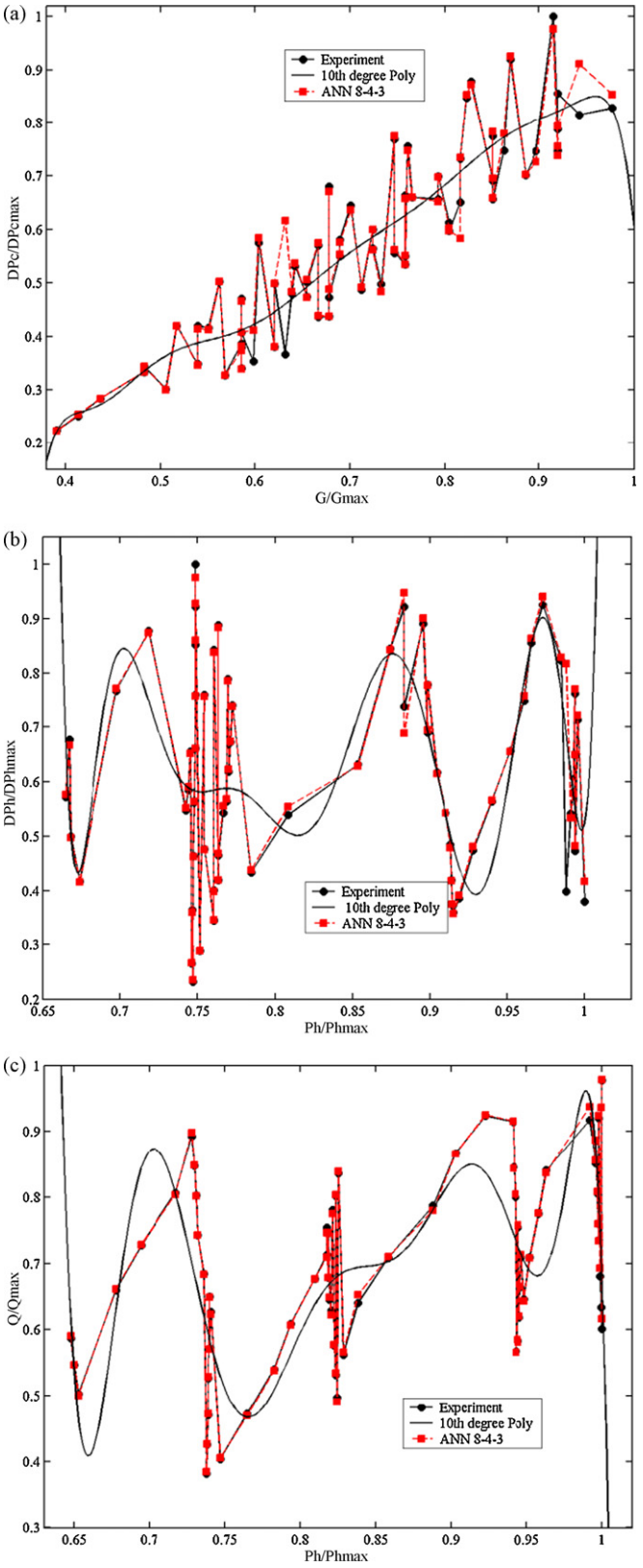

Fig. 17. The second example: the comparisons of ANN 8–4–3 vs. 10th order PF for: (a) cold-sided pressure drop, (b) hot-sided pressure drop and (c) heat transfer.

Table 6
Total error comparisons.

Network vs. polynomial	Total error
ANN 8–4–1 (q''_w output)	0.32930703
Polynomial fitting of 10th order (q''_w output)	2.29901621
ANN 8–4–3 (DP_c output)	0.08875032
Polynomial fitting of 10th order (DP_c output)	0.360642
ANN 8–4–3 (DP_h output)	0.18246256
Polynomial fitting of 10th order (DP_h output)	1.645394
ANN 8–4–3 (Q output)	0.093324986
Polynomial fitting of 10th order (Q output)	2.056541

mial for ΔP_c, ΔP_h, and Q were 0.360642000, 1.645394000, and 2.056541000, respectively whereas those of ANN 8–4–3 which had the poorest performance were only 0.088750320, 0.182462560, and 0.093324986, for three different output variables modeled (ΔP_c, ΔP_h, and Q, respectively). The ANN approach clearly yields more representative results. Thus, if the parameter space for an engineered thermal system component is designed to work under non-linear load and/or in conjunction with significant changes in the 'equation of state', then the above described ANN approach can facilitate the design and analysis tasks.

5. Conclusion

The paper presents the EBaLM algorithm, a combination of two neural network training methods, the error-back propagation and the Levenberg–Marquard algorithms. The EBaLM algorithm was tested on two different thermohydraulic reference problems. The first was convective heat transfer of supercritical CO_2 through a single tube and the second on convective heat transfer in a multi-zig-zagged channel printed circuit heat exchanger. Further, a comparison was made between the ANN algorithm EBaLM and a 10th order polynomial fit. The neural network approach performed better than the polynomial fit; the latter could not mimic the given, oscillatory nature of the reference data. In the first example, the performance of a 20 neural architecture divided into 4 groups and 5 different neural configurations was investigated. In the second example, four neural network architectures were investigated and applied to predict thermohydraulics of PCHE.

The results revealed that all of the ANN architectures were in good agreement with the referenced conditions. In fact, even though the reference data was fluctuating and oscillatory, the neural network was able to follow these characteristic changes. It is evident that the advantage of neural network approach is the network's ability to learn the dataset. In contrast, a polynomial fit is at best able to follow the stepwise average of the oscillatory nature of the reference dataset. Thus at each step, it fails to fully capture nature of both the non-linearity and 'noise' contained in experimental data. In fact, the total error of a 10th order polynomial fit was one to three orders of magnitude larger than that associated with the neural networks. As substantiated in Table 6, even the relatively poor simulation of the ANN 8–4–3 architecture showed a figure of merit two orders of magnitude better in terms of *TE* than the 10th order polynomial (0.093324986 vs. 2.056541 for the output Q).

The engineering task of designing an advanced nuclear system with systems, subsystems and components optimized for performance while in regulatory compliance requires a tremendous effort and iteration-intensive engineering design. We are thus interested in considering methods and/or practices that may reduce the trial-and-error in design optimization. Thus, if the parameter space for a thermal system component is designed to work under non-linear load and/or in conjunction with significant changes in the thermophysical 'equation of state', then the above described approach may facilitate the design engineering process.

Acknowledgements

The authors would like to thank University of Idaho and Debbie McQueen for their support. Further, the first and third authors express their gratitude for support provided under DOE NERI and DE-FC07-05ID14672.

References

Boroushaki, M., Ghofrani, M.B., Lucas, C., 2005. Simulation of nuclear reactor core kinetics using multilayer 3-D cellular neural network. IEEE Trans. Nucl. Sci. 52, 719–728.
Diaz, G., Sen, M., 1999. Simulation of heat exchanger performance by artificial neural network. HVAC R Res. 5, 195–208.
Ermis, K., 2007. ANN modeling of compact heat exchanger. Int. J. Energy Res. 32, 581–594.
Eryurek, E., Upadhyaya, B.R., 1990. Sensor validation for power plants using adaptive backpropagation neural network. IEEE Trans. Nucl. Sci. 37, 1040–1047.
Feay, D.A., 1994. Compact heat exchanger: a review of current equipment and R&D in the field. Heat Recover Syst. CHP 14, 459–474.
Garg, A., Sastry, P.S., Pandey, M., Dixit, U.S., Gupta, S.K., 2007. Numerical simulation and artificial neural network modeling of natural circulation boiling water reactor. Nucl. Eng. Des. 237, 230–239.
Guanghui, S., Morita, K., Fukuda, K., Pidduck, M., Dounan, J., Miettinen, J., 2003. Analysis of the critical heat flux in round vertical tubes under low pressure and flow oscillation conditions. Applications of artificial neural network. Nucl. Eng. Des. 220, 17–35.
Guo, Z., Uhrig, R.E., 1992. Nuclear power plant performance study by using neural network. IEEE Trans. Nucl. Sci. 39, 915–918.
He, S., Jiang, P.X., Xu, Y.J., Shi, R.F., Kim, W.S., Jackson, J.D., 2005. A computational study of convection heat transfer to CO_2 at supercritical pressures in a vertical mini tube. Int. J. Therm. Sci. 44, 521–530.
Heatric Website: http://www.heatric.com URL from March 2008.
Incropera, F.P., Dewitt, D.P., Bergman, T.L., Lavine, A.S., 2007. Fundamentals of Heat and Mass Transfer. Johns Wiley & Sons, New Jersey.
Ishizuka, T., Kato, Y., Muto, Y., Nikitin, K., Ngo, T.L., 2005. Thermal–hydraulic characteristics of a printed circuit heat exchanger in supercritical CO_2 loop. In: The 11th International Topical Meeting on Nucleus Reactor Thermal–Hydraulics, Pops' Palace Conference Center, Avignon, France, October 2–6.
Levenberg, K., 1944. A method for the solution of certain problems in least square. Quart. Appl. Math. 2, 164–168.
Li, X., Pierres, R.L., Dewson, S.J., 2006. Heat exchangers for the next generation of nuclear reactors. In: Proceedings of the ICAPP'06, Reno, NV, USA, June 4–8.
Lillo, T. M., June 2005. Analysis Methods and Desired Outcomes of the Analysis of Intermediate Process Heat Exchanger Loop Requires. INL/EXT-05-00478, Idaho National Laboratory.
Lomperski, S., Cho, D., Song, H., Tokuhiro, A., 2006. Testing of a compact heat exchanger for use as the cooler in a supercritical CO_2 Brayton cycle. In: Proceedings of the ICAPP'06, Reno, NV, USA, June 4–8.
Marquardt, D., 1944. An algorithm for least-squares estimation of nonlinear parameters. SIAM J. Appl. Math. 11, 431–441.
Mi, Y., Tosoukalas, L.H., Ishii, M., Li, M., Xiao, Z., 1996. Hybrid fuzzy-neural flow identification methodology. In: Proceedings of the Fifth IEEE International Conference on Fuzzy System, New Orleans, LA, September 8–11.
Mi, Y., Ishii, M., Tosoukalas, L.H., 1998. Vertical two-phase flow identification using advanced instrumentation and neural networks. Nucl. Eng. Des. 184, 409–420.
Mi, Y., Ishii, M., Tosoukalas, L.H., 2001. Flow regime identification methodology with neural networks and two-phase flow models. Nucl. Eng. Des. 204, 87–100.
Minsky, M., Papert, S., 1969. Perceptron. MIT Press, Cambridge.
Nikitin, K., Kato, Y., Ngo, L., 2006. Printed circuit heat exchanger thermal–hydraulic performance in supercritical CO_2 experimental loop. Int. J. Refrig. 29, 807–814.
NIST website: http://webbook.nist.gov/chemistry/fluid/URL from March 2008.
Pacheco-Vega, A.J., 2001. Neural network analysis of fin-tube refrigerating heat exchanger with limited experimental data. Int. J. Heat Mass Transf. 44, 763–770.
Pacheco-Vega, A.J., 2002. Simulation of compact heat exchangers using global regression and soft computer. Ph.D. Dissertation. Depart. Aero. and Mech. Eng., Univ. of Notre Dame, Notre Dame, Indiana.
Ping, H., Ling, X., 2008. Optimal design approach for the pate-fin heat exchanger using neural networks cooperated with genetic algorithms. Appl. Therm. Eng. 28, 642–650.
Roh, M.-S., Cheon, S.-W., Chang, S.-H., 1991. Thermal power prediction of nuclear power plant using neural network and parity space model. IEEE Trans. Nucl. Sci. 38, 866–872.
Schultz, R.R., Nigg, D.W., September 2004. Next Generation Nuclear Plant-Design Methods Development and Validation Research and Development Program Plan. INEEL/EXT-04-02293. Idaho National Engineering and Environmental Laboratory.

Shah, R.K., Sekulic, D.P., 2003. Fundamentals of Heat Exchanger Design. Johns Wiley & Sons, New Jersey.
Song, H., Meter, J.V., Lomperski, S., Cho, D., Kim, H.Y., Tokuhiro, A., 2006. Experimental investigations of a printed circuit heat exchanger for supercritical CO_2 and water heat exchanger. In: Fifth Korea-Japan Symposium on Nuclear Thermal Hydraulics and Safety, Jeju, Korea, November 26–29.
Song, H., 2007. Investigations of a printed circuit heat exchanger for supercritical CO_2 and water. M.S. Thesis. Mech. Eng., Kansas State Univ., Manhattan, Kansas.
Southworth, F.H., MacDonald, P.E., Harrell, D.J., Shaber, E.L., Park, C.V., Holbrook, M.R., Petti, D.A., November 2003. The Next Generation Nuclear Plant (NGNP) Project. INEEL/CON-03-01150, Preprint. Idaho National Engineering and Environmental Laboratory.
Tsoukalas, L.H., Uhrig, R.E., 1997. Fuzzy and Neural Approaches in Engineering. Johns Wiley & Sons, New Jersey.
Tsuzuki, N., Kato, Y., Ishiduka, T., 2007. High performance printed circuit heat exchanger. Appl. Therm. Eng. 27, 1702–1707.
Van Meter, J., 2008. Experiment investigation of a printed circuit heat exchanger using supercritical carbon dioxide and dioxide and water as heat transfer media. M.S. Thesis. Nucl. Eng., Kansas State Univ., Manhattan, Kansas.
Vaziri, N., Hojabri, A., Erfani, A., Monsefi, M., Nilforooshan, B., 2007. Critical heat flux prediction by using radial basis function and multilayer perceptron neural network: a comparison study. Nucl. Eng. Des. 237, 377–385.
Werbos, P.J., 1994. The Roots of Backpropagation. Johns Wiley & Sons, New York.
Zurada, J.M., 1992. Introduction to Artificial Neural Systems. West Publishing, Minnesota.